Mario Collepardi Symposium

on

Advances in Concrete Science and Technology

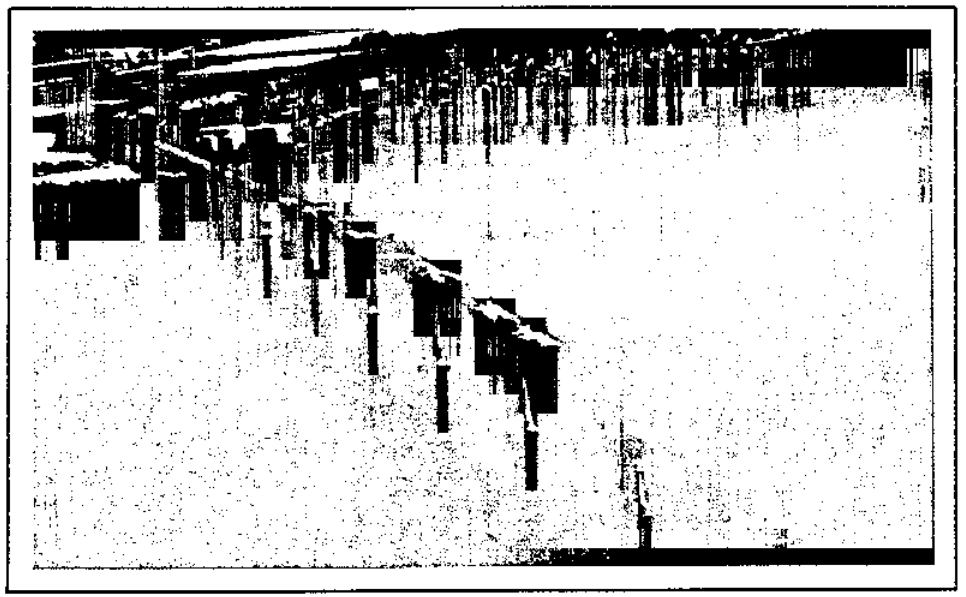

P.K. Mehta
Editor

Design of Reinforced High Strength Concrete Structures

By L. Coppola

Synopsis: High Strength Concrete (*HSC*) is characterized by physical, elastic and mechanical properties which are significantly different from those of Normal Strength Concrete (*NSC*). From the civil engineering point of view, compressive strength alone is not sufficient by itself to design reinforced concrete structures. Other properties, such as drying shrinkage, creep, modulus of elasticity, Poisson's ratio, tensile and flexural strength are also needed for a safe design of concrete structures.

Relationships between the above mentioned properties and the compressive strength are available in codes or norms for *NSC* in form of equations or tables based on consolidated experimental data. On the other hand, these relationships can change from *NSC* to *HSC* as a function of the compressive strength itself. The analysis of codes and norms of *HSC* has shown how for the application of this material it has been necessary to change the existing relationships between these concrete properties and compressive strength. Moreover for *HSC* the relationship between elastic modulus or tensile strength on one hand, and compressive strength on the other, significantly changes from one code to another. Therefore there is the need to concentrate the research efforts to identify the factors that determine the considerable variation of the elastic-mechanical properties of *HSC*.

High strength concrete is characterized by a higher brittleness compared to *NSC*. However, a fragile behavior of the material by itself does not necessarily correspond to an equally brittle behavior of the reinforced concrete structures. Therefore, it is just as important to concentrate the research efforts to have more realistic data for the design of the reinforced high strength concrete members. There is the need to direct the research on *HSC* not simply on the peculiar features of the material per se but, above all, on the aspects of the design of reinforced members. In fact, the concrete behavior can be substantially changed by the interaction with the reinforcement. The lack of knowledge about these interactions forces the various codes to adopt too much restrictive requirements that presently reduce the advantages of using *HSC* in structural applications.

Keywords: Compressive strength, tensile strength, modulus of elasticity, Poisson's ratio, drying shrinkage, creep, stress-strain relationship.

Luigi Coppola is a research civil engineer and technical director of Enco, Spresiano, Italy. He has authored numerous papers on various aspects of concrete technology, durability and mix-design.

1. INTRODUCTION

Until a few decades ago *High Strength Concrete* (*HSC*) was exclusively a matter of research in technologically advanced laboratories. However, in the last ten years the development and use of this material have undergone a considerable increase. *HSC* has been widely used in the construction of off-shore structures and long span bridges in the North of Europe (1) where, due to the exceptional loads in service and the severe environmental conditions, it was impossible to use *Normal Strength Concrete* (*NSC*). Furthermore *HSC* has been used profitably in high-rise buildings to limit the size of the columns at the lower floors (2). *HSC* has also been applied in precast structures, bridge superstructures and in the field of nuclear wastes (3-6).

The ease with which 100 N/mm^2 compressive strength concretes are manufactured may be attributed to the following factors:

- superior quality of portland cement characterized by a higher content of tricalcium silicate (C_3S), the component that contributes the most to the strength, and by a higher cement fineness;
- the advent of superplasticizers that allows for the reduction of the water-cement ratio without any decrease in concrete workability (7);
- the availability of silica fume which, with its finer particles (< 0.1 μm), reduces the cement paste porosity and improves the quality of the transition zone in terms of higher bond strength between the cement matrix and the aggregate surface (8).

Owing to the technological developments, the term *HSC* has taken on a different meaning over the years. For example, in the 1950s in the USA, *HSC* was considered to be a concrete with a compressive strength of only 35 N/mm^2 (9). However, by the 1960s concrete with a compressive strength of about 45 N/mm^2 was used commercially. In the 1970s-1980s concretes with compressive strength of 70 N/mm^2 were used in various structures including, for instance, the columns of the *Interfirst Plaza* built in Dallas in 1983. Presently, in the USA concretes with compressive strength higher than 75 N/mm^2 are employed for the construction of high-rise buildings.

In Europe the definition of *HSC* is not the same in every country. However, according to the CEB-FIP Working Group (10), *HSC* is understood to be that which has characteristic compressive strength higher than that normed by the domestic standard codes in each country (about 60 N/mm^2).

High strength concretes have physical, elastic and mechanical properties which are substantially different from those of normal concrete which has a compressive strength in the range of 25-40 N/mm^2.

From the civil engineering point of view, compressive strength alone is not sufficient by itself to design reinforced concrete structures. Other properties, such as drying shrinkage, creep, modulus of elasticity, Poisson's ratio, tensile and flexural strength are also needed for a safe design of concrete structures. Relationships between the above mentioned properties and the compressive strength are available in codes or norms for *NSC* in form of equations or tables based on consolidated experimental data. On the other hand, these relationships can change from *NSC* to *HSC* as a function of the compressive strength itself. Moreover, there is some uncertainty on these relationships for *HSC* due to the lack of experimental data which are not as numerous and thorough as for *NSC*. The main purpose of the present paper is to examine comparatively these relationships for *HSC* as available in codes or norms of different countries, particularly in Europe and North America. An other important purpose of this paper is to examine the design criteria which should be adopted to mitigate or eliminate some intrinsic drawbacks of these materials, related specifically to the high strength level: for instance, although the stress-strain behavior of *HSC* is typically that of a brittle material, ductile concrete structures can be manufactured by using adequate and properly designed metallic reinforcements.

2. PHYSICAL, ELASTIC AND MECHANICAL PROPERTIES OF HSC

In this section, some of the fundamental properties of *HSC*, such as stress-strain behavior, elastic modulus, Poisson's ratio, tensile strength, etc., will be analyzed. Moreover, relationships between compressive strength and these fundamental properties of *HSC* - which are generally different from those of normal concretes - will be presented.

2.1 Stress-Strain Behavior

The stress-strain behavior (Fig. 1) of *HSC* has been widely studied (11-13). Its most significant aspects, compared to *NSC*, are:

- a more linear shape of the stress-strain curve to a higher percentage of the maximum stress;
- a slightly higher strain at maximum stress;
- a steeper shape of the descending part of the curve and a lower ultimate strain, which both indicate a marked brittleness of the material.

The stress-strain behavior of *HSC* can be attributed nearly exclusively to the improvement of the mechanical properties of the cement paste-aggregate

interface (transition zone). The porosity of the latter is lower as a result of the decrease of the internal bleeding, which is owed to the presence of silica fume. The increase of the bond-strength in the transition zone implies a reduced amount of microcraking at lower levels of loading. This explains the more linear shape of the ascending part of the stress-strain curve.

Microcracking occurs at the cement paste-aggregate interface of *NSC* when the stress is equal to 65% of the compressive strength (11). On the contrary, in *HSC* this occurs when the stress is equal to 80% of the compressive strength.

To explain the shape of the descending part of the curve, it must be remembered that concrete is basically composed of cement paste and aggregates. Although both of these components are brittle materials, normal strength concrete shows a relatively ductile behavior as a result of the large difference in the rigidity of the cement matrix and aggregates (Fig. 2a). In fact the *E*-modulus of the cement paste generally varies between 15000 and 35000 N/mm^2, whereas the *E*-modulus of the aggregates is generally higher than 50000 N/mm^2. This difference causes a stress concentration at the interface which promotes a crack formation. As the stress increases, part of the energy is consumed when the crack pattern develops. At this stage, due to the slip of the cracks in the cement paste, the stress-strain curve deviates considerably from the linear elastic course. After the ultimate stress has been reached, the microcracks provide an efficient redistribution of the internal stress and, hence, a tough failure.

In *HSC* the difference between the *E*-modulus of the cement paste and that of the aggregates is considerably lower (Fig. 2b). This clearly provides a more homogeneous stress distribution and consequently a lower possibility of microcracking at the interface. A less developed microcracking pattern provides a lower redistribution of the stress and, therefore, a brittle failure of high strength concrete.

According to this model, the stress-strain behavior of the concrete is strictly influenced by the *E*-modulus of the aggregates. Aggregates having an *E*-modulus which is similar to that of the cement paste (Fig. 3, gneiss: E = 40000 N/mm^2), lead to a higher strain at maximum stress and a more brittle failure. On the contrary, aggregates having a much superior *E*-modulus compared to that of the cement paste (Fig. 3 bauxite: E = 100000 N/mm^2) provide a more ductile behavior.

2.2 Modulus of Elasticity and Poisson's Ratio

Numerous experimental tests (14-16) have demonstrated that the rise in the elastic modulus is very slight as the compressive strength increases. Therefore, the relationships available in standards and codes valid for the normal strength concretes, which permit the calculation of the *E*-modulus for a given compressive strength, cannot be used for the calculation of the *E*-modulus in

HSC. These relationships in fact tend to overestimate the *E*-modulus of concretes having compressive strengths higher than 40-50 N/mm^2.

In the extension, published in 1995, to the European CEB-FIP Model Code 90 (17-18) the equation:

$$E_{ci} = 10^4 (f_{ck} + 8)^{1/3} \qquad [1]$$

valid for normal strength concrete with a compressive strength lower than 50 N/mm^2, is replaced by the equation:

$$E_{ci} = 22000 [(f_{ck} + 8)/10]^{0.3} \qquad [2]$$

or:

$$E_{ci} = 22000 [f_{cm}/10]^{0.3} \qquad [3]$$

where E_{ci} = tangential elastic-modulus

f_{ck} = cylinder characteristic compressive strength

f_{cm} = cylinder mean compressive strength

The above mentioned equations [2-3] can also be used for normal strength concretes.

Table 1 reports the values of *E*-modulus calculated by equation [2] as a function of the cylinder characteristic compressive strength.

The experimental data indicate that no substantial differences exist between Poisson's ratio (measured in the elastic range) between *NSC* and *HSC*. The values of Poisson's ratio vary generally between 0.18 and 0.24 as a function of the applied stress (19). On the contrary, in the inelastic range *HSC* seems to have a lower lateral strain compared to *NSC*. This effect is due to the lower microcracking pattern at the cement paste-aggregate interface. On the other hand the lower lateral strain is responsible for a lower increase of the ultimate compressive strength compared to *NSC*, with confining lateral pressure.

It is well known that the increase in compressive strength of columns (Δf_c) caused by an idealized lateral confining pressure (σ_3) can be quantified through a "confinement" factor *K*:

$$\Delta f_c = K\sigma_3 \qquad [4]$$

For *NSC*, *K* is equal to 4.0; for *HSC* it has been proposed to adopt a value equal to 2.8 (20). In other words, spirals and rectangular hoop ties are less effective in confining *HSC* core compared to their effect on a low-medium strength core. Furthermore, some experimental data (21-22) seem to indicate a decrease of the ultimate strain and an increase in the slope of the descending part of the stress-strain curve for *HSC* columns with lateral steel confinement.

Therefore we are able to conclude that to obtain *HSC* columns with the same ductile behavior as low strength concrete columns it is necessary to increase the amount of confinement reinforcement.

2.3 Tensile Strength

Just like the *E*-modulus, tensile strength increases very little with compressive strength: if the compressive strength doubles, the increase of the tensile strength is of about 20%. Furthermore, according to some data (23), the splitting tensile strength in *NSC* is about 10% of the compressive strength of the material, whereas in *NSC* the splitting tensile strength is reduced to just 5% of the compressive strength.

The extension (18) to the CEB-FIP Model Code 1990 (17) proposes to employ the following formulae for the calculation of tensile strength:

$$f_{ctk,min} = 1.22\ [(f_{ck} + 8)/18]^{0.6} \qquad [5]$$

$$f_{ctk,max} = 2.38\ [(f_{ck} + 8)/18]^{0.6} \qquad [6]$$

$$f_{ctm} = 1.80\ [(f_{ck} + 8)/18]^{0.6} \qquad [7]$$

where $f_{ckt,min}$, $f_{ckt,max}$ are the characteristic tensile strength corresponding to 5% and 95% fractiles respectively, and f_{ctm} is the mean tensile strength.

Table 2 shows values of the tensile strength, calculated by employing these formulae, as a function of the cylinder characteristic compressive strength.

2.4 Shrinkage

The data available on concrete shrinkage seem to indicate a shrinkage rate immediately after exposure to a dry environment which is greater for *HSC* than for *NSC* (24). However, generally, in the long term, after 4 months, the differences in the shrinkage values between *HSC* and *NSC* are not substantial (25). The low water-cement ratio which characterizes the *HSC* is responsible for the phenomenon of self-desiccation of cement paste which, with the refinement of the porosity dispersed in the microstructure, determines a greater autogenous shrinkage compared to *NSC*. The lower the water-binder ratio the more this phenomenon takes place. The true drying shrinkage, however, is much less due to the lack of evaporable water, compared to *NSC*. The two above mentioned phenomena seem to compensate each other, as the total shrinkage of *HSC* and *NSC* is practically the same.

Moreover, some results (23) seem to indicate that the shrinkage of *HSC* depends more on the water content in the mixture than on the water-cement

ratio. These results could explain why *HSC*, obtained by reducing the water-cement ratio through an increase of the binder factor, but without any reduction of water in the mixture, gives higher shrinkage values than *NSC* (26).

Lastly, it is necessary to underline how the microcracking pattern induced by shrinkage in structures made of *HSC* is worse than in those made of *NSC*. The formation of cracks occurs immediately following demoulding, and, in the case of *HSC*, appears to be related to the greater shrinkage rate, the higher *E*-modulus, the reduced creep (paragraph 2.5), and the lack of aggregates interlock in the cracks of *HSC* (27). While the first three factors determine an increase in the tensile stress caused by shrinkage, the lack of an interlock mechanism reduces the concrete resistance to crack formation.

2.5 Creep

The experimental data (28, 29) indicate that creep in *HSC* (manufactured with superplasticizers to limit the cement factor) is noticeably lower compared to that of *NSC* (Fig. 4).

In Fig. 5 it is possible to assess the influence of the stress-strength ratio on the creep coefficient, which is the multiplicative coefficient employed to calculate the creep from the elastic strain. As can be seen, for a stress value between 40 and 80% of the compressive strength, the creep coefficient - registered during a loading time from 28 to 70 days - is significantly lower for *HSC* (22).

It is important to point out that although the experimental data available seem to show that the creep is lower for *HSC* than for *NSC*, the working group that has prepared the extension (18) to the CEB-FIP Model Code '90 did not reach a unanimous agreement on this subject. Therefore, they have referred the task of analyzing the behavior of *HSC* under sustained loads to a special committee.

3. CODES AND NORMS

In this paragraph some of the available codes and norms on *HSC* are examined. Generally these codes and norms were developed first in countries such as Canada , Norway, Finland etc, where the environmental conditions are so severe that the use of *HSC* became necessary due to durability reasons rather than for real structural needs.

These codes and norms will be compared with the extension to the CEB-FIP Model Code '90 which has already been mentioned in this paper in the paragraphs on *E*-modulus and on tensile strength.

3.1 The Finnish Code

The Finnish Code and in particular the 1991 DBY34 supplement of the RAK MK B4 1983/94 Code states that it is possible to use *HSC* with cube characteristic compressive strength higher than 60 N/mm^2 (concrete grade: K60), but lower than 100 N/mm^2 (K100). In this code the most significant physical, elastic, and mechanical parameters are determined as follows:

- cylinder characteristics compressive strength (f_{ck}) is obtained by multiplying *K* by 0.7;
- the tensile strength for concrete grade K70, K80, K90, K100 is equal to 3.3, 3.5, 3.7 and 3.90 N/mm^2 respectively;
- the *E*-modulus is equal to 38700 N/mm^2 independently of the concrete grade;
- creep is assumed to be 30% lower than that of a concrete mixture having a water content lower than 170 kg/m^3;
- the stress-strain relationships selected for the ultimate limit state design are those shown in Fig. 6.

The stress-strain relationships in Fig. 6 are made up of three segments. The first one, from the origin to 0.6 f_{ck}, has a slope corresponding to an *E*-modulus equal to 38750 N/mm^2. The second segment starts from 0.6 f_{ck} and reaches the point of co-ordinates (ε_{co}, f_{ck}). The last segment is horizontal and reaches the co-ordinate point (ε_{cu}, f_{ck}). The values of ε_{co} and ε_{cu} (strain at maximum stress and ultimate strain respectively) both depend on f_{ck}. The ε_{co} value is equal to 0.18% and 0.22% for K60 and K100 respectively; the ε_{cu} value is equal to 0.35 and 0.27% for the same K values. The Code also states that in verifying the structure for shear, the designer must employ the properties of a concrete with K = 60 regardless of the quality of the concrete actually employed (30). This limitation is probably due to the lack of the interlock mechanism, proved by the breakage of the aggregates in the tensile splitting tests (31).

3.2 Norwegian Codes

Norwegian Codes NS 3473 of 1992 permit the use of *HSC* with a cube characteristic compressive strength (f_{ck})* of 105 N/mm^2 (concrete grade: C105).

It is interesting to observe that the Norwegian Norms introduce the concept of in situ compressive strength (f_{cn}), which is calculated through the following equation:

*It must be pointed out that the symbol f_{ck} used in the Norwegian Norms to indicate the cube characteristic compressive strength is the same one employed in other norms (e.g. the Finnish one) for the cylinder characteristic compressive strength.

$$f_{cn} = f_{ck} \cdot 0.56 + 2.8 \qquad [8]$$

The design compressive strength (f_{cn}) can be determined from in situ compressive strength using a safety factor (γ_m) which is equal to 1.4:

$$f_{cd} = f_{cn}/\gamma_m = f_{cn}/1.4 \qquad [9]$$

Figure 7 shows the schematic stress-strain behavior of *HSC* according to the Norwegian Norms. The strain values (ε_{cn}, ε_{co}, ε_{cu}) in Fig. 7 can be calculated by the following equations:

$$\varepsilon_{cn} = f_{cn}/E_{cn} = f_{cn}/[9500\,(f_{cn})^{0.3}] \qquad [10]$$

$$\varepsilon_{co} = (0.004\,f_{cn} + 1.9) \cdot 10^{-3} \qquad [11]$$

$$\varepsilon_{cu} = (2.5m - 1.5)\,\varepsilon_{cn} = (2.5\varepsilon_{co}/\varepsilon_{cn} - 1.5)\,\varepsilon_{cn} \qquad [12]$$

The equations [10-12] are strictly valid for $f_{ck} \leq 85$ N/mm^2. The values of E_{cn} and ε_{co} for concrete having a compressive strength greater than 85 N/mm^2 must be determined experimentally.

The values of σ_{cn} in Fig. 7 can be obtained from the following equations:

$$\sigma_{cn} = E_{cn}\,\varepsilon_c \qquad \text{for } 0 < \varepsilon_c < 0.6\,f_{cn}/E_{cn} \qquad [13]$$

$$\sigma_{cn} = E_{cn}\,\varepsilon_c + f_{cn}\,(m\text{-}1)\left[\frac{E_{cn}\varepsilon_c + 0.6\,f_{cn}}{(0.6 - m)f_{cn}}\right]^{\frac{m-0.6}{m-1}} \qquad \text{for } 0.6\,f_{cn}/E_{cn} \leq \varepsilon_c < \varepsilon_{co} \qquad [14]$$

$$\sigma_{cn} = f_{cn} \qquad \text{for } \varepsilon_{co} \leq \varepsilon_c < \varepsilon_{cn} \qquad [15]$$

Figure 8 shows the stress-strain curves for ultimate limit state design according to the Norwegian Norms.

Table 5 shows values of the characteristic tensile strength (f_{tk}) and of the in situ tensile strength (f_{tn}) for concrete grades ranging from 25 to 105 N/mm^2. It is interesting to notice that the in situ tensile strength doesn't vary when f_{ck} is higher than 85 N/mm^2. The design tensile strength f_{td} can be obtained dividing (f_{tn}) by 1.4 ($f_{td} = f_{tn}/1.4$).

3.3 Dutch Norms

In the supplement of the Dutch Norms NEN 6720, NEN 5950 and NEN 6722 the use of 105 N/mm^2 cube characteristic compressive strength (f_{cck})

concrete is allowed. The design compressive strength (f_{cd}) can be calculated from this value as follows:

$$f_{cd} = K\, f_{cck}/\gamma_c \qquad [16]$$

where: γ_c is a safety factor equal to 1.2 and K is a reduction factor which takes into account both the difference between cube strength and cylinder strength and the creep due to sustained loads. It is calculated through the following equation:

$$K = (785 - f_{cck})/1000 \qquad [17]$$

The stress-strain relationships for ultimate limit state design (Fig. 9) are essentially made up of two segments: The first one, which represents the ascending portion of the curve up to a strain ε_{c1}, is characterized by the E_c elastic modulus:

$$E_c = 35900 + 40\, f_{cck} \qquad [18]$$

The second segment is horizontal with ordinates equal to f_{cd} and maximum abscissa equal to ε_{cu}. The values of ε_{c1} and ε_{cu} are shown in Table 4.

In the shear resistance calculation, the design tensile strength ($f_{ctd} = f_{ctk}/1.4$) is assumed to be that which corresponds to a concrete with $f_{cck} = 65$ N/mm^2, regardless of the actual compressive strength:

$$f_{ctd} = f_{ctk}/1.4 = 0.7\,(3 + 0.02\, f_{cck})/1.4 \qquad [19]$$

3.4 USA Norms

In the USA Norms (*ACI 318-89 "Building Code Requirements for Concrete Structures"*) there are no limitations to the cylinder compressive strength (f'_c) except for the calculation of concrete contribution to shear strength. In this case the maximum compressive strength is limited to 70 N/mm^2.

Design compressive strength (f_{cd}) can be calculated as follows:

$$f_{cd} = \left(f'_c\right) 0.85\, \varnothing \qquad [20]$$

where $\varnothing$, is a strength reduction factor ranging from 0.7 to 0.9 directly related to the strength of the structural members: for instance, it is equal to 0.75 for structural members reinforced by a spiral confinement, and loaded in compression and flexure; $\varnothing$ is equal to 0.85 for members subjected to shear

and torsion. The coefficient 0.85 in equation [20] takes into account the difference in compressive strength between specimen and structure.

The stress-strain relationship must be based on results of comprehensive tests. Furthermore, the USA Norms permit the adoption of an equivalent rectangular compressive stress distribution (stress block) to replace the more exact concrete stress distribution. In the rectangular stress block a constant stress f_c ($f_c = \alpha_1\, f'_c = 0.85\, f'_c$) is assumed uniformly distributed over an equivalent compression zone bounded by edges of the cross section and a straight line located parallel to the neutral axis at a distance $a = \beta_1 \cdot c$ from the fiber of maximum compressive strain. The c symbol is the distance of the neutral axis from the fiber of maximum compressive strain and β_1 is a coefficient equal to 0.85 for $f'_c \le 30$ N/mm^2. It decreases continuously at a rate of 0.05 for each 7 N/mm^2 in excess of 30 N/mm^2, but not lower than 0.65. Basically, the USA Norms by means of this factor, take into account a more triangular stress-strain curve of *HSC* compared to *NSC*.

The concrete ultimate strain is equal to 0.3%. The *E*-modulus (E_c) is calculated from the following formula:

$$E_c = 4700\, \sqrt{f'_c} \qquad [21]$$

However, it must be taken into consideration that this equation overestimates the *E*-modulus of concretes with compressive strength higher than 40 N/mm^2 compared to the actual values. Therefore, ACI Committee 363 suggests the following formula to calculate the *E*-modulus:

$$E_c = 3320\, \sqrt{f'_c} + 6900 \qquad [22]$$

Lastly, for the modulus of rupture (f_r) the following equation is proposed:

$$f_r = 0.59\, \sqrt{f'_c} \qquad [23]$$

3.5 Canadian Norms

The Canadian Norms *CSA A23.3.94* (1994) permit the use of concretes with a cylinder compressive strength up to 80 N/mm^2. Overall, the relationship to calculate the tensile strength and the elastic modulus are substantially equal to those suggested by the ACI Standards. The concrete ultimate strain is equal to 0.35%.

The same conclusions are adopted relative to the stress-strain curve and the rectangular stress block. However, different equations are used to calculate the parameters which identify the stress block. In particular, the Canadian Norms confirm the decrease in β_1 coefficient ($\beta_1 = 0.97\text{-}0.0025\, f'_c \ge 0.67$). At the same

time these norms impose that the factor α_1, which in the ACI recommendation is constant and equal to 0.85, decreases as the compressive strength increases according to the following equation:

$$\alpha_1 = 0.85 - 0.0015\ f_c' \geq 0.67 \qquad [24]$$

The reduction of α_1 takes into account the differences in the stress-strain curves between *NSC* and *HSC*. Furthermore, the decrease of α_1 considers the difference between compressive strength measured on specimens and on structural members. The reduction of α_1, also suggested by other norms (for example New Zealand), still seems to be a subject of controversy as the ACI has confirmed the constant value (0.85) for α_1.

3.6 The New Zealand Norms

The New Zealand Code *NZS 3101* (1995) is substantially the same as the ACI except for the calculation of the coefficients α_1 and β_1 which identify the stress block. The New Zealand Code claims that the coefficients α_1 and β_1 proposed by the ACI lead to an overestimation of the member capacity. Therefore, the New Zealand Code suggests the adoption of the following formulae for α_1 and β_1:

$$\alpha_1 = 0.85 \qquad \text{for } f_c' \leq 55 \text{ N/mm}^2$$

$$\alpha_1 = 0.85 - 0.004\,(f_c' - 55) \geq 0.75 \qquad \text{for } f_c' > 55 \text{ N/mm}^2 \qquad [25]$$

$$\beta_1 = 0.85 \qquad \text{for } f_c' \leq 30 \text{ N/mm}^2$$

$$\beta_1 = 0.85 - 0.008\,(f_c' - 30) \geq 0.65 \qquad \text{for } f_c' > 30 \text{ N/mm}^2 \qquad [26]$$

3.7 The Extension to the CEB-FIP Model Code 1990

In 1995 an extension to the CEB-FIP Model Code 1990 appeared in CEB Bulletin No. 228 (18). The aim of the working group was to critically analyze the possibility to extend the design criteria of Code 90 valid only for *NSC* ($f_{ck} \leq 50\text{N/mm}^2$) to *HSC* ($50 < f_{ck} \leq 100$ N/mm^2).

The most important modifications of the CEB-FIP Model Code '90 regard the safety factor of the concrete (γ_c) which is 1.5 for *NSC*. Given the high brittleness of *HSC*, this value has been increased using a multiplicative factor (γ_{hsc}):

$$\gamma_{hsc} = 1/(1.1 - f_{ck}/500) \qquad [27]$$

Factor γ_{hsc} is equal to 1 or 1.11 when f_{ck} is equal to 50 or 100 N/mm^2, respectively. Therefore γ_c is equal to 1.5 or 1.66 when f_{ck} equals 50 or 100 N/mm^2, respectively.

Moreover, a stress-strain diagram has been tendered for strength check in the ultimate limit states under axial and flexure load. This diagram (Fig. 10) is characterized by a curve that from the axis origin reaches the point ε_{c1} (strain at maximum stress) and is then completed by a horizontal line to point ε_{cu} (ultimate strain). The parameters describing the ascending part of the curve (σ_{cd}, n) and the values ε_{c1} and ε_{cu} can be determined, as a function of f_{ck}, through the following equations:

$$\sigma_{cd} = 0.85\ f_{cd}\,[1-[1-(\varepsilon_c/\varepsilon_{c1})]^n] \qquad [28]$$

$$n = 2 - 0.008\,(f_{ck} - 50) \qquad [29]$$

$$\varepsilon_{c1} = 0.002 + 0.5\,(f_{ck} - 50)\cdot 10^{-5} \qquad [30]$$

$$\varepsilon_{cu} = 0.0025 + 0.002\,(1 - f_{ck}/100) \qquad [31]$$

In the calculation of the shear capacity, the code confirms the validity of the equation used for *NSC* because this formula is in itself quite safe:

$$f_{cd2} = 0.60\,(1 - f_{ck}/250)\cdot f_{cd} \qquad [32]$$

where f_{cd2} is the concrete contribution to the shear strength.

3.8 The German Norms

The German Norms (*DAfStb - Richtlinie für hochfesten Beton*, 1995) permit the use of concrete with cube characteristic compressive strength (β_{WN}) up to 115 N/mm^2 (concrete grade: B115). However, the elastic and mechanical properties of concretes with a characteristic compressive strength higher than 95 N/mm^2 (B95) must be examined beforehand with experimental tests. In Table 5 the *E*-modulus (E_b) values are shown for the different concrete grades.

The parameters for the stress-strain curve are shown in Table 6: ε_{bs} and ε_{bu} are the strain at maximum stress and the ultimate strain, respectively. The β_R value is the design compressive strength equal to $0.69\,(1-\beta_{WN}/600)\,\beta_{WN}$.

From the data given in Table 6 it can be seen that the ascending part of the stress-strain curve has the same structure as the formula [28] proposed by the extension to the CEB-FIP Model Code:

$$\sigma_c = \beta_R[1-(1-\varepsilon_b/\varepsilon_{bs})^n] \qquad [33]$$

4. CONSIDERATIONS AND SUGGESTIONS ON THE CODES FOR HSC

Some considerations on the most significant characteristics of *HSC* such as *E*-modulus, tensile strength, stress-strain behavior, and safety factor can be made based on the examination of the previously mentioned codes.

Figure 11 highlights the considerable variation in the elastic modulus at a given compressive strength from one code to another. There is a difference of about 40% between the maximum and minimum values for the same compressive strength level.

Figure 12 shows the relationships between tensile strength and compressive strength according to the different codes. Again, at equal compressive strength, there is a significant variation in the tensile strength calculated through the formulae proposed by the different codes. For instance, the tensile strength values according to the Canadian Norms are 60% of those determined by CEB-FIP Model Code (18). Consequently, recommended values for the minimum reinforcement ratio for bending and shear vary significantly from one code to another (32).

Brittle failure which characterizes *HSC* determines considerable difficulties in recording the strain-softening branch of the stress-strain curve. Consequently there are not many experimental data for the stress-strain relationship. Therefore, the analytical formulations of the complete stress-strain curve for *HSC* are continuously changing as new data become available (33-38). However, the experimental results and the numerical simulations at present both highlight two particular aspects of *HSC*: the decrease in the ultimate strain and a steeper descending branch of the stress-strain curve, both proving the brittle behavior of *HSC* (39). In spite of this behavior, the USA, Canadian and New Zealand Codes use a constant value for the ultimate strain for both *HSC* and *NSC*. On the contrary, the other codes consider a decrease in the plastic strain as the compressive strength increases taking into account the higher brittleness of *HSC*. Moreover, these codes use stress-strain analytical formulations, that determine strain values which are safer than those obtained in experimental tests (40-41).

The USA, Canadian and New Zealand Codes permit the adoption of a simplified procedure for the integration of the stress-strain curve. This procedure is based on the definition of a rectangular stress block. However, there are differences in the stress block in the ACI Code on one hand, and the Canadian or New Zealand Norms on the other. The ACI Codes define a stress block characterized by a constant value of the stress (equal to $\alpha_1 f'_c = 0.85 f'_c$) regardless of the concrete compressive strength. On the contrary, the Canadian and New Zealand Norms suggest a reduction in the stress level by decreasing the factor α_1 as the concrete compressive strength increases. In fact, it has been demonstrated that the adoption of a constant stress level in the ACI recommendation can lead to an overestimation of the ultimate strength of the

members (32, 42). As a matter of fact the Canadian and New Zealand Norms agree with the concept adopted by German, and European Norms, which recommend a reduction of the design strength by increasing the safety factor (γ_c). Basically, it can be assumed that the coefficient α_1 of the Canadian Norm is equivalent to $1/\gamma_c$ in the German and European Norms.

The extension to the CEB-FIP Model Code '90 and the German Norm suggest a rise of the γ_c value as the compressive strength increases. The difference in the γ_c values between the two above mentioned norms consists exclusively in the initial values (lower in the German Norm) whereas the increase rate in γ_c is substantially equal for German and CEB-FIP Norms (39). In particular, the safety factor values vary between 1.15 and 1.28 in the German Norm. The extension to the CEB-FIP Model Code, instead, assumes γ_c values much higher, ranging between 1.5 and 1.66. The increase in the safety factor as the compressive strength rises, as well as the reduction in the ultimate strain imposed by the CEB-FIP Model Code, considerably reduce the advantages of using *HSC*. Figure 13 shows the axial load-moment interaction diagram for concrete grades 50 to 90 calculated using the CEB-FIP stress-strain relationship. These diagrams refer to a symmetrically reinforced rectangular cross section beam (reinforcement ratio 0.53; width = 300 mm; height = 500 mm). The Figure shows that the different curves do not undergo a substantial enlargement as the f_{ck} values increase from 50 to 90 N/mm^2.

Contrarily, the German Norms favor an improved use of *HSC* by adopting a lower safety factor than that imposed in the CEB-FIP Model Code. For example, in Fig. 14 it can be seen how the axial load-moment interaction diagram of the above mentioned beam, for concretes with the same characteristic compressive strength (f_{ck} = 85 N/mm^2), is noticeably wider using the German Norm compared to the CEB-FIP Model Code.

The reason why the CEB-FIP Model Code increased the safety factor is based on the higher brittleness of *HSC*. This reasoning does not seem to take into account the differences existing between the behavior of the concrete by itself and that of the reinforced member. In fact, the increase of γ_c alone cannot represent a satisfactory answer to safety in terms of member toughness. Therefore, the problem of toughness in reinforced structures must be faced by defining some design aspects such as the reinforcement ratio, the form and distribution of the transversal reinforcement, rather than the mere increase of the safety factor.

On the whole, it can be concluded that the definition of the stress-strain relationship of the material is not sufficient to understand the structural behavior of the reinforced concrete members. The analysis of the reinforced rectangular cross section beam subjected to flexure allows to comment on this assumption.

Figure 15 (39) shows the adimensional ultimate curvature (χ^*) of the section as a function of the mechanical reinforcement ratio (ω). By increasing the

concrete compressive strength, the point that identifies the change in the failure mode of the member (due to steel or concrete) moves towards a lower mechanical reinforcement ratio. Furthermore, in the region where the failure is caused by the concrete, the increase in the compressive strength determines a sharp decrease of the ultimate curvature and consequently of the ductility for the same ω value. However, an increase in the concrete compressive strength allows the design of sections with lower mechanical reinforcement ratio also for high geometrical reinforcement ratio (ρ) and thus characterized by tough failure. At a given geometrical reinforcement ratio, there is an increase in the ultimate curvature of the section as the concrete compressive strength rises (Fig. 16). This behavior confirms that the brittleness of the material does not necessarily determine a brittle failure of the structure (39). Unfortunately, the marked reduction in the ultimate strain imposed by various codes impedes the change of the brittle failure into a tough failure through an increase in the concrete compressive strength.

In members subjected to axial load with flexure the advantages of using *HSC* are considerably less. This is due to the fact that the failure mode depends on the stress level and on the ultimate curvature of the concrete, but it is substantially independent of the reinforcement ratio. In this case, in fact, the mode of section failure can be modified only by changing the sizes of the section (39).

5. CONCLUSIONS

HSC is characterized by physical, elastic and mechanical properties which are significantly different from those of *NSC*.

The analysis of codes and norms of *HSC* has shown how for the application of this material it has been necessary to change the existing relationships between some concrete properties and compressive strength. Moreover, for *HSC* the relationship between elastic modulus or tensile strength on one hand, and compressive strength on the other, significantly changes from one code to another. Therefore there is the need to concentrate the research efforts to identify the factors that determine the considerable variation of the elastic-mechanical properties of *HSC*.

High Strength Concrete is characterized by a higher brittleness compared to *NSC*. However a fragile behavior of the material by itself does not necessarily correspond to an equally brittle behavior of the reinforced concrete structures. Therefore, it is just as important to concentrate the research efforts to have more realistic data for the design of the reinforced concrete members. That is to say that there is the need to direct the research on *HSC* not simply on the peculiar features of the material per se but, above all, on the aspects of the design of reinforced members. In fact, the concrete behavior can be

substantially changed by the interaction with the reinforcement. The lack of knowledge about these interactions forces the various codes to adopt excessively restrictive requirements that presently reduce the advantages of using *HSC* in structural applications.

ACKNOWLEDGMENT

Helpful comments in calculating the interaction diagrams by Alessandro Panizzo were very valuable in the preparation of the final draft.

The work in preparing the text and Figures by Alessandra Galletti and Mara Meneghel is acknowledged.

REFERENCES

(1) Larsen, T., and Helland, S., "Experience from the Use of High Strength Concrete on 3 Sites in Norway", Proceedings of the 1st Int. Symposium on the Utilization of High Strength Concrete, Stavanger, Norway (1987), pp. 517-526.

(2) Chicago Committee on High-Rise Buildings, "High-Strength Concrete in Chicago High-Rise Buildings", Task Force Report No. 5, 1977, 63 pp.

(3) Matsumoto, Y., et al. "Precast Prestressed Concrete Truss Railway Bridge using Extremely High Strength Concrete", Final Report, 10th IABSE Congress Tokio, (1976), pp. 433-438.

(4) Helland, S., "High Strength Concrete used in Highway Pavements", Proceedings of the 2nd Int. Symposium on the Utilization of High Performance Concrete, Berkeley, USA (1990).

(5) Coppola, L., Troli, R., Cerulli, T., and Collepardi, M., "The Influence of Raw Materials on the Performance of Reactive Powder Concrete", Proceedings of the International Congress on High Performance Concrete, and Performance and Quality of Concrete Structures, Florianopolis, Brazil (1996), pp. 502-513.

(6) Torrenti, S.M., Matte, V., Maret, V., and Richet, C., "High Integrity Containers for Interim Storage of Nuclear Wastes Using Reactive Powder Concrete", Proceedings of the Fourth Int. Symposium of the Utilization of High Strength/High Performance Concrete, Paris, France (1996), pp. 1407-1413.

(7) Collepardi, M., and Ramachandran, V.S., "Effect of Admixtures", Proceedings of the 9th International Congress on the Chemistry of Cement, Vol. I, Theme III D, New Delhi, India (1992).

(8) Bache, H.H., "Densified Cement/Ultra-Fine Particle Based Materials", 2nd Int. Conference on Superplasticizers in Concrete, Ottawa, Canada (1981), 35 pp.

(9) Russel, H.G., "High Stregth Concrete in North America", Proceedings of the 1st Int. Symnposium on the Utilization of High Strength Concrete, Stavanger, Norway (1987), pp. 561-572.

(10) FIP-CEB Working Group, "High Strength Concrete. State of the Art Report", August (1990).

(11) Carrasquillo, R.L., Slate, F.O., and Nilson, A.H., "Microcraking and Behaviour of HSC subject to Short-Term Loading", ACI-Journal, Proceedings V. 78, No. 3, May-June (1981), pp. 179-186.

(12) Tognon, G., Ursella, P., and Coppetti, G., "Design and Properties of Concretes with Strength over 1500 kg/cm^2", ACI-Journal, Proceedings V. 77, No. 3, May-June (1981), pp. 171-178.

(13) Smeplass, S., Justenes, H., Sellevold, E.J., and Ronning, T.,"Results from the Norwegian Research Project: Materialutvikling Hoyfast Betong", Report available from the Cement and Concrete Research Institute, Trondheim (1990).

(14) Carrasquillo, R.L., Slate, F.O., and Nilson, A.H., "Properties of High Strength Concrete Subjected to Short-Term Loads", ACI-Journal, Proceedings V. 78, No. 3, May-June (1981), pp. 171-178.

(15) Bernhardt, and Hoff, "Hoyfast betong", Delrapport 0. Forsok med bjelder i hoyfast betong "HSC", SINTEF report STF65 A85021.

(16) Hoiseth, Hoff, and Jensen, "Hoyfast betong", Delrapport 2. Soyler under sentrisk last. SINTEF report STF65 A83049.

(17) CEB Bulletin d'Information n° 203, "CEB-FIP Model Code 1990", Final Draft, July (1991).

(18) CEB Bulletin d'Information n° 228, "High Performance Concrete. Recommended Extensions to the Model Code 90. Research Needs", July (1995).

(19) Ahmad, S., and Shah, S.P., "High Strength Concrete - A Review." First symposium on Utilization of High Strength Concrete, Stavanger, Norway, June (1987),pp. 255-268.

(20) Jensen, J. J., and Bjerkeli, L., "Effect of water pressure on concrete structures. Water absorption, static strength and strain development tests", SINTEF report STF65 F87037.

(21) Martinez, S., Nilson, A.H., and Slate, F.O., "Spirally Reinforced High Strength Concrete Columns", ACI Journal, Proceedings V. 81, No. 5, Sept-Oct. 1984, pp.431-442.

(22) Bjerkeli, L., Tomaszewicz, A. and Jensen, J.J., "Deformation Properties and Ductility of High Strength Concrete", Proceedings of the Second International Symposium on Applications of High Strength Concrete, Berkeley, 1990.

(23) State-of-the-art-report on High Strength Concrete. Reported by ACI Committee 363, ACI Journal, Proceedings V. 81, July-August 1984, pp. 362-411.

(24) Tomaszewicz, A., Bynboe, J., and Jensen, J.J., Hoyfast betong. Delrapport 5. Pilotforsok med kryp i hoyfast betong. SINTEF report STF65 A 85006.

(25) Charif, H., Jaccoud, J.P., and Alou, F., "Reduction of Deformations with the Use of Concrete Admixtures", Proceedings of the RILEM Symposium on Admixture for Concrete, Barcelona, May (1990), pp. 402-428, Ed. E. Vazquez.

(26) Parrott, L.J., "The Production and Properties of High Strength Concrete", Concrete, V. 3, No. 11, November (1969), pp. 443-448.

(27) Wiegrink, K., Marikunte, S., and Shah, S.P., "Shrinkage Cracking of High Strength Concrete", ACI Materials Journal, Sept.-Oct. 1996, pp. 409-415.

(28) Russell, H.G., and Corley, W.G.,"Time Dependent Behavior of Columns in Water Tower Place", Douglas McHenry International Symposium on Concrete and Concrete Structures, SP-55, American Concrete Institute, Detroit, (1978), pp. 347-373.

(29) Ngab, A.S., Slate, F.O., and Nilson, A.H., "Behavior of High Strength Concrete Under Sustained Compressive Stress", Research Report No. 80-2, Department of Structural Engineering, Cornell University, Ithaca, February (1980), 201 pp.

(30) CEB Bulletin d'Information N°222, "Application of High Perfomance Concrete", November (1994).

(31) P. Marro, "High-Strength Concrete Structures: Design Codes, and Applications" (in Italian), Proceedings of the Congress "L'Evoluzione nella sperimentazione per le costruzioni", Malta (1996), pp. 163-184.

(32) Paultre, P., "Beton a Hautes performances. Reglements Etrangers", Bullettin del Laboratories del Ponts ed Chaussees, Special XIX, pp. 131-150.

(33) Ahmad, S.H., and Shah, S.P., "Structural Properties of High-Strength Concrete and its Implication for Precast Prestressed Concrete", PCI Journal, Vol. 30, n° 6, (1985), pp. 92-119.

(34) Cusson, D., and Paultre, P., "Experimental Study of High Strength Concrete Columns Confined by Rectangular Ties", Proceedings of the Symposium on the Utilization of High-Strength Concrete, Lillehammer, Norway, (1993), pp. 137-144.

(35) Cusson, D., and Paultre, P., "Stress-Strain Model for Confined High Strength Concrete", ASCE, Journal of Structural Engineering, Vol. 121, n° 3, (1995), pp. 468-477.

(36) Tomaszewicz, A., "Betongens Arbeidsdiagram", SINTEF Report n° STF 65A 84065, Trondheim, (1984).

(37) Collins, P., "Structural Design Considerations for High-Strength Concrete", Network of Centres of Excellence on High Performance Concrete, Toronto, October 4-7 (1992).

(38) Van Gysel, A., and Taerwe, L., "Analytical Formulation of the Complete Stress-Strain Curve for High Strength Concrete", Materials and Structures, Vol. 29, November (1996), pp. 529-533.

(39) Fabbrocino, G., and Pecce, M., "Some Considerations about the Stress-Strain Behaviour for High-Strength Concretes" (in Italian), Enclosed in Industria Italiana del Cemento, 3, (1996), pp. 3-7.

(40) Kaar, P.H., Hanson, N.W., and Capell, H.T., "Stress-Strain Characteristics of High Strength Concrete", ACI Special Pubblication SP 55, Detroit, USA, (1978), pp. 161-185.

(41) Muguruma, H., Nishiyama, M., and Watanabe, F., "Stress-Strain Curve Model for Concrete with a Wide Range of Compressive Strength", Proceedings of the Symposium on the Utilization of High Strength Concrete, Lillehammer, Norway (1993), pp. 314-321.

(42) Hibrahim, H.H.H., and MacGregor, J.G., "Flexural Behavior of High-Strength Concrete Columns", Research Report 196, Department of Civil Engineering, University of Alberta, Edmonton, Canada, (1994), 197 pp.

Table 1 - Tangential E-modulus for concretes with different f_{ck}

f_{ck} (N/mm^2)	12	20	30	40	50	60	70	80	90	100
E_{ci} (N/mm^2) $\cdot 10^3$	27	30	33	35	37	39	41	42	44	45

Table 2 - Tensile strength for concretes with different f_{ck}.

f_{ck} (N/mm^2)	12	20	30	40	50	60	70	80	90	100
f_{ctm} (N/mm^2)	1.9	2.3	2.8	3.2	3.6	4.0	4.4	4.7	5.0	5.3
$f_{ctk,min}$ (N/mm^2)	1.3	1.6	1.9	2.2	2.5	2.7	3.0	3.2	3.4	3.6
$f_{ctk,max}$ (N/mm^2)	2.5	3.1	3.7	4.3	4.8	5.3	5.8	6.2	6.6	7.0

Table 3 - Characteristic and in situ tensile strength for concretes with different f_{ck} according to the Norwegian Norms.

f_{ck} (N/mm^2)	25	35	45	55	65	75	85	95	105
f_{tk} (N/mm^2)	2.1	2.55	2.95	3.3	3.65	4.0	4.3	4.6	4.9
f_{in} (N/mm^2)	1.4	1.7	2.0	2.25	2.50	2.60	2.7	2.7	2.7

Table 4 - Strain at maximum stress and ultimate strain for concretes with different f_{cck} according to the Dutch Norms.

f_{cck} (N/mm^2)	65	75	85	95	105
ε_{c1} (%)	0.175	0.175	0.180	0.185	0.190
ε_{cu} (%)	0.350	0.325	0.300	0.275	0.250

Table 5 - E-modulus for different concrete grades according to the German Norms.

β_{WN} (N/mm^2)	65	75	85	95	105	115
E_b (N/mm^2)	40500	42000	43000	44000	44500	45000

Table 6 - Parameters for stress-strain curve according to the German Norms.

β_{WN}(N/mm^2)	65	75	85	95	105	115
β_R (N/mm^2)	40	45	50	55	60	64
ε_{bx} (%)	0.203	0.206	0.210	0.214	0.217	0.220
ε_{bu} (%)	0.310	0.270	0.250	0.240	0.230	0.220
n*	2.0	1.9	1.8	1.7	1.6	1.55

*see equation [33]

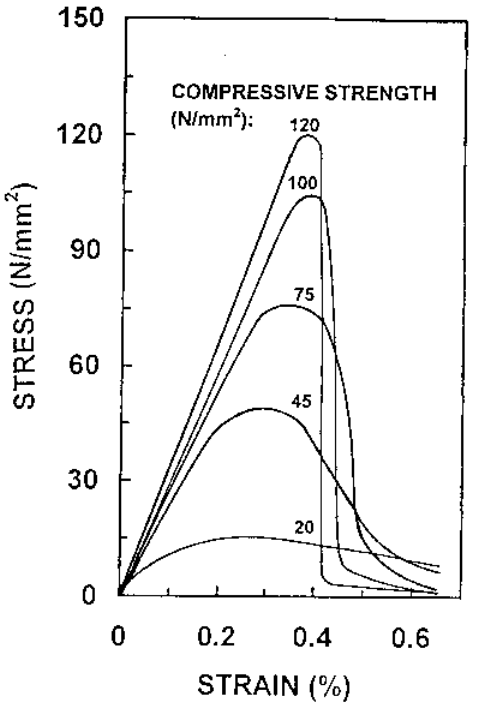

Fig. 1 - Stress-strain behavior of HSC compared to NSC.

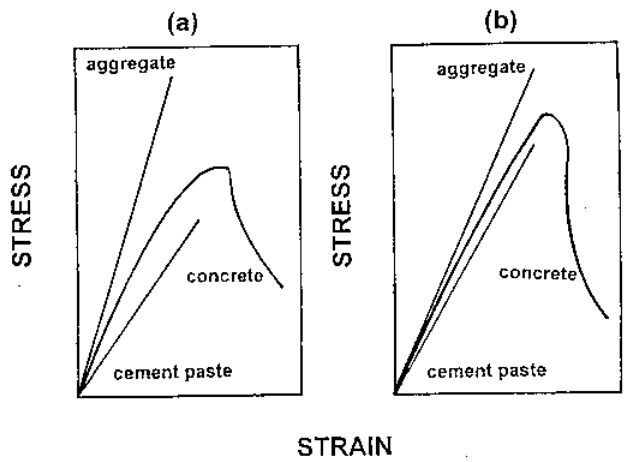

Fig. 2 - Schematic stress-strain behavior of cement paste, aggregate, normal (a) and high strength concrete (b).

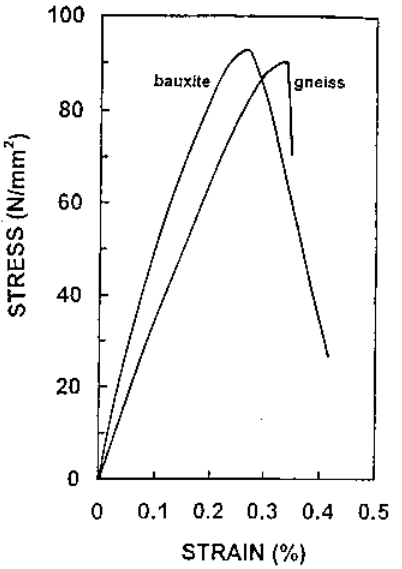

Fig. 3 - Stress-strain behavior of concretes having the same compressive strength manufactured with different *E*-modulus aggregates (bauxite or gneiss).

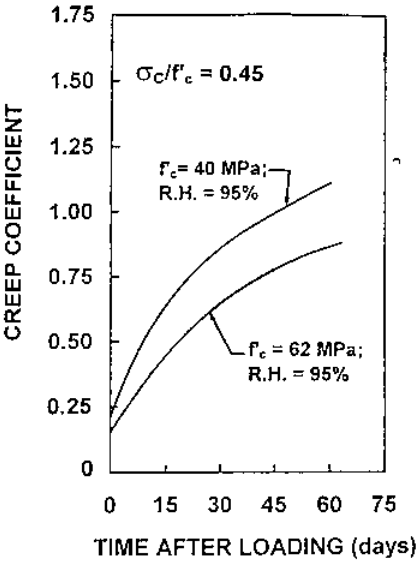

Fig. 4 - Creep coefficient as a function of time after loading for concretes with different compressive strengths (f'_c).

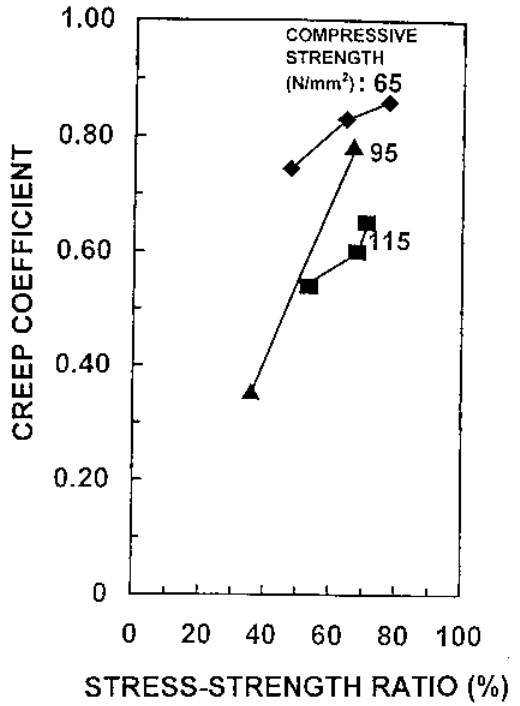

Fig. 5 - Relationship between creep coefficient and stress levels for different concretes.

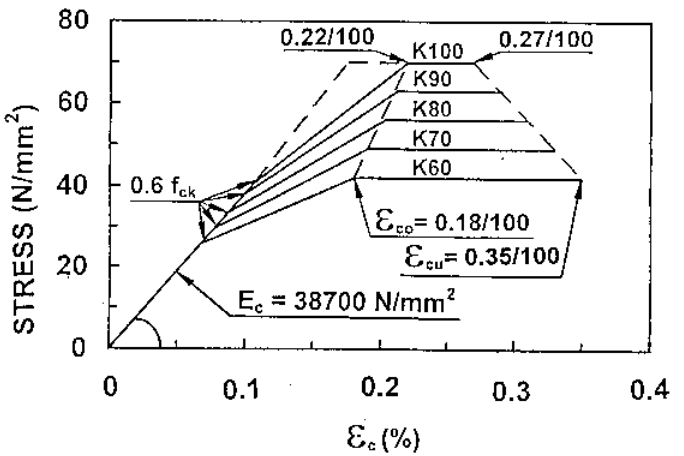

Fig. 6 - Stress-strain behavior of HSC according to the Finnish Norms.

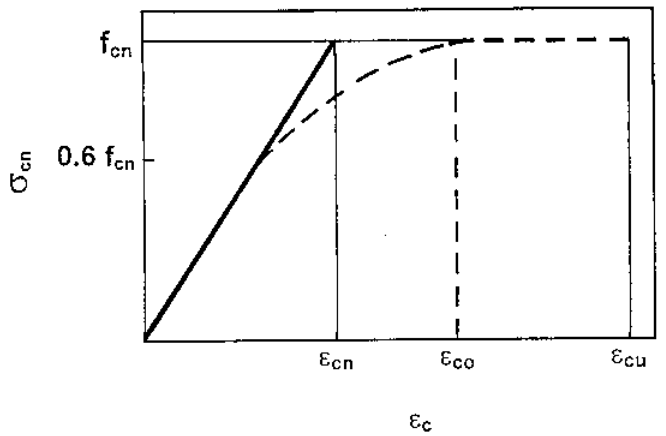

Fig. 7 - Schematic stress-strain curves according to the Norwegian Norms.

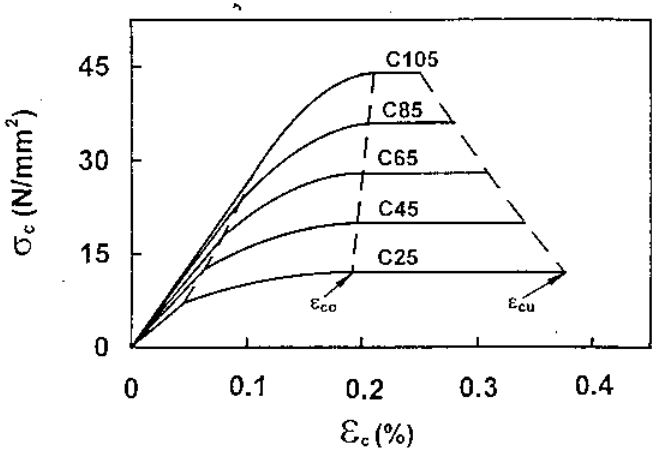

Fig. 8 - Stress-strain diagrams according to the Norwegian Norms.

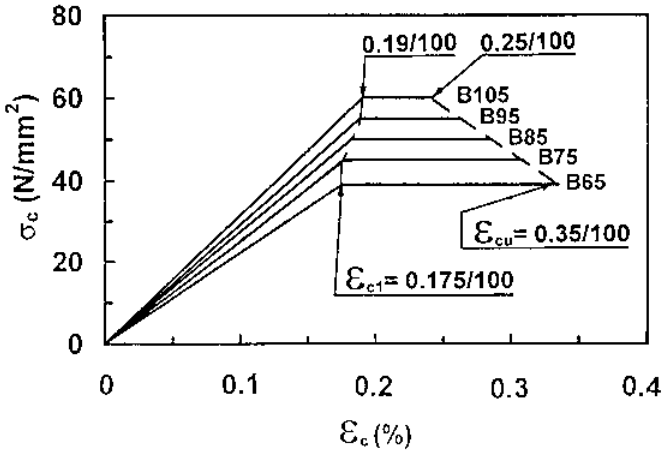

Fig. 9 - Stress-strain behavior according to the Dutch Norms.

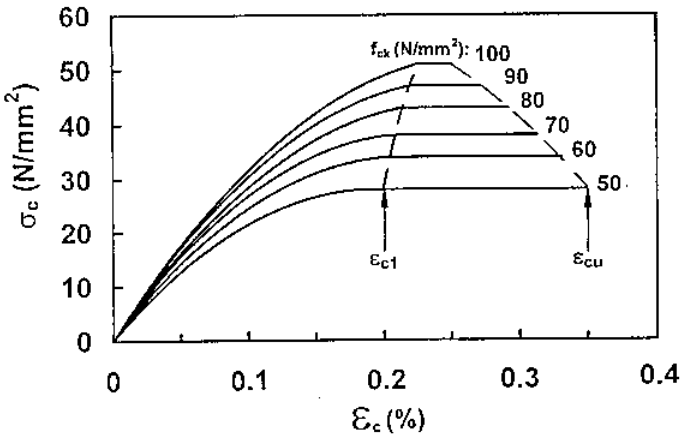

Fig. 10 - Stress-strain behavior according to the extension to the CEB-FIP Model Code 1990.

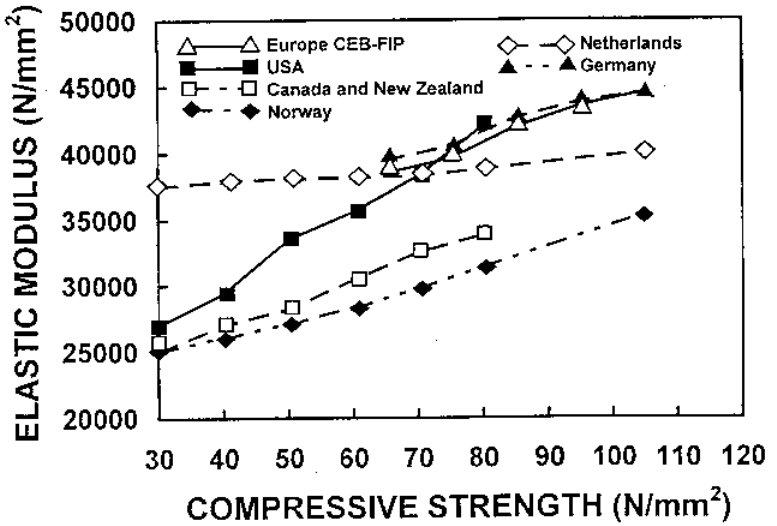

Fig. 11 - E-modulus versus compressive strength according to different codes.

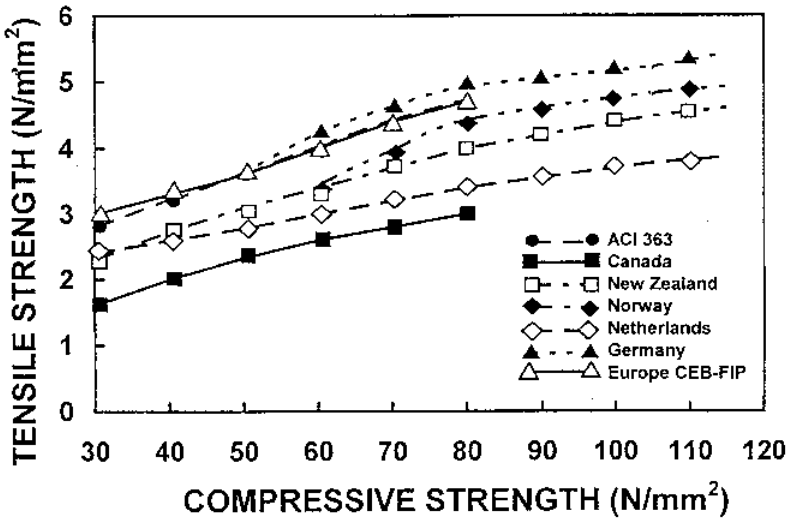

Fig. 12 - Tensile strength versus compressive strength according to different codes.

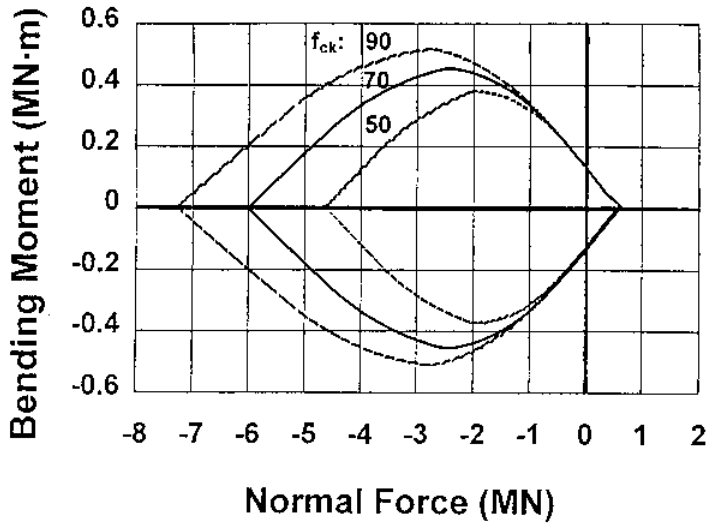

Fig. 13 - Axial load - moment interaction diagrams for a reinforced beam for different concrete grades (according to CEB-FIP).

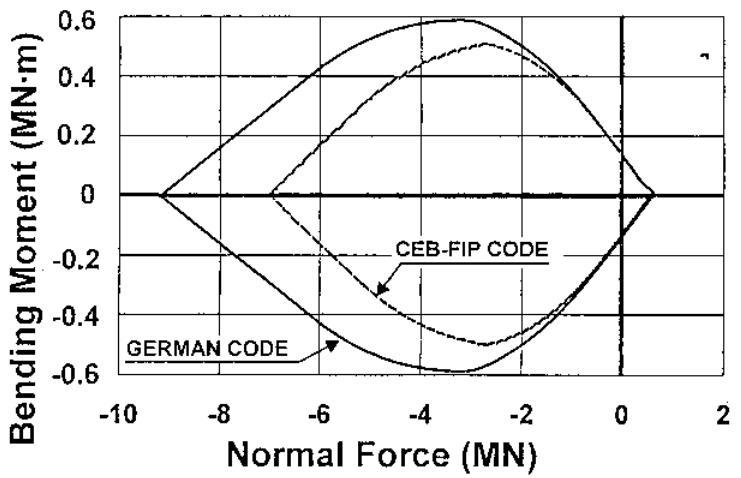

Fig. 14 - Axial load - moment interaction diagrams for a reinforced beam according to CEB-FIP or German Norms (f_{ck}=85 N/mm²).

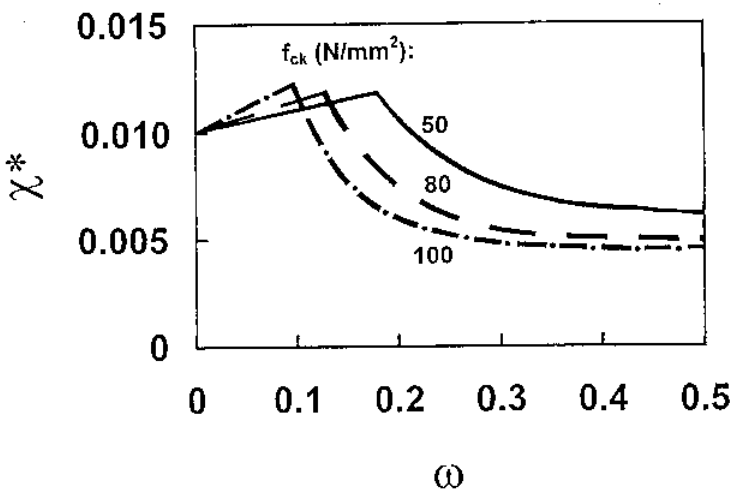

Fig. 15 - Adimensional ultimate curvature (χ^*) versus mechanical reinforcement ratio (ω), according to CEB-FIP.

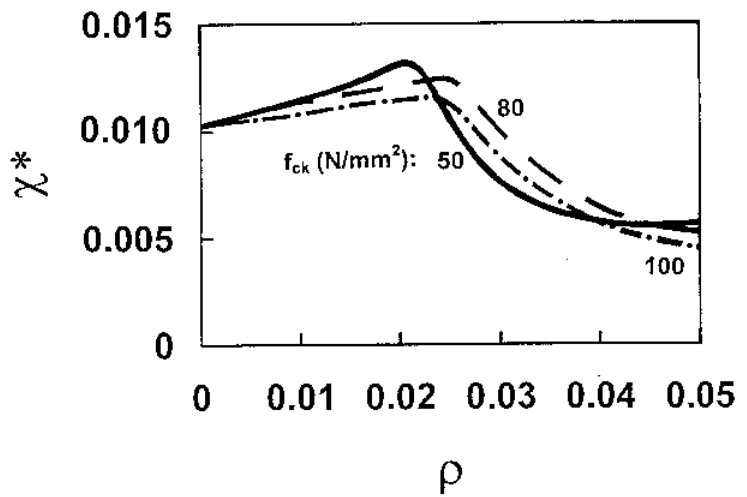

Fig. 16 - Adimensional ultimate curvature (χ^*) versus geometrical reinforcement ratio (ρ), according to CEB-FIP.